# HYBRID NEURAL LUMPED ELEMENT APPROACH
# IN INVERSE MODELING OF RF MEMS SWITCHES

## Tomislav Ćirić[1], Zlatica Marinković[1], Rohan Dhuri[2], Olivera Pronić-Rančić[1], Vera Marković[1]

[1]University of Niš, Faculty of Electronic Engineering, Niš, Serbia
[2] ALTEN GmbH, Munich, Germany

**Abstract**. *RF MEMS switches have been efficiently exploited in various applications in communication systems. As the dimensions of the switch bridge influence the switch behaviour, during the design of a switch it is necessary to perform inverse modeling, i.e. to determine the bridge dimensions to ensure the desired switch characteristics, such as the resonant frequency. In this paper a novel inverse modeling approach based on combination of artificial neural networks and a lumped element circuit model has been considered. This approach allows determination of the bridge fingered part length for the given resonant frequency and the bridge solid part length, generating at the same time values of the elements of the switch lumped element model. Validity of the model is demonstrated by appropriate numerical examples.*

**Key words**: *Artificial neural networks, inverse modeling, lumped element model, RF MEMS switch.*

## 1. INTRODUCTION

Radio-Frequency Micro-Electro-Mechanical Systems (RF MEMS) components have been proven to be of a great importance for RF circuits and subsystems, as they possess characteristics that may surpass characteristics of conventional, purely electrical components. RF MEMS devices consist of moving sub-millimeter-sized parts that provide radio frequency functionality. They are of high linearity, low insertion loss and extremely good intermodulation performance. MEMS devices have the ability to sense, control and actuate on micro scale, and generate effects on macro scale. According to variety and diversity of RF MEMS technology functionalities, they have wide applicability for the new generation of communication system components, like switches and varactors (variable capacitors), resonators, complex networks, reconfigurable filters, phase shifters, impedance matching tuners and programmable step attenuators [1-9]. In the recent time, the RF MEMS technology has found applications for Internet of Things (IoT), Internet of Everything (IoE), Tactile Internet and 5G telecommunications [10-12]. Design of the

circuits containing RF MEMS switches requires repeated simulations and/or optimizations of the switch characteristics. Therefore, there is a need for reliable RF MEMS models. Switch electrical characteristics can be accurately determined in full-wave electromagnetic simulators [13-15]. However, as the simulation models are quite complex and the simulations consume a significant amount of time, a common option to overcome these problems is usage of lumped models in the circuit simulators [16, 17]. The lumped element models based on the equivalent circuits are faster than the full-wave ones. However, if differently sized bridges are analyzed, the procedures for obtaining the equivalent circuit elements have to be repeated, which is a time-consuming process. To make the lumped element model scalable with the dimensions, artificial neural networks (ANNs) were proposed to model the dependence of the lumped element model on the switch bridge dimensions [18]. The switch bridge dimensions determine the electromagnetic characteristics of the switch. Therefore during the design of a switch, it is necessary to determine the bridge dimensions to ensure the desired switch characteristics, such as resonant frequency, i.e. to perform the inverse modeling of the switch. The authors of this work proposed earlier a black-box inverse modeling of the RF MEMS capacitive switches where the bridge lateral dimensions were determined for given electrical or mechanical switches [19-25]. In this work, the neural based inverse modeling approach is extended in a way that the novel approach provides not only determination of the bridge dimensions but also the values of the corresponding lumped model elements, resulting in a lumped element model ready to be used for further simulations of the circuits containing the considered switch.

The paper is organized as follows: after Introduction, a description of the considered RF MEMS switch is given in Section 2. The proposed modeling approach is described in Section 3. Details of the model development and validation and the most illustrative numerical results are given is Section 4. Section 5 contains the conclusions.

## 2. RF MEMS CAPACITIVE SWITCHES

MEMS are integrated devices consisting of micromechanical and electronic components. RF MEMS switches are the specific micromechanical switches that are designed to operate at RF to mm-wave frequencies. RF MEMS switches use mechanical movements of the bridge to achieve a closed or open circuit in the RF transmission lines. RF MEMS classification depends on the type of actuation, deflection axis, contact type, circuit configuration, and structure configuration. The considered device is a Coplanar waveguide (CPW) based RF MEMS capacitive shunt switch (Fig. 1(a)) designed at Fondazione Bruno Kessler (FBK) in Trento in an 8 layer Silicon micromachining process [26-28].

The device is fabricated on silicon substrate and silicon dioxide ($SiO_2$) as insulator. The bridge is a thin gold (Au) membrane connecting both sides of the ground plane with defined lateral dimensions (length of the fingered part - $L_f$ and length of solid part – $L_s$).

The signal line is a thin aluminum layer, placed below the bridge. On the opposite sides of the signal line, the DC actuation pads made of polysilicon are placed. Applying the actuation voltage on electrodes, electrostatic force becomes superior over mechanical restoring force, causes membrane to pull down towards the ground plane switching the circuit [26].
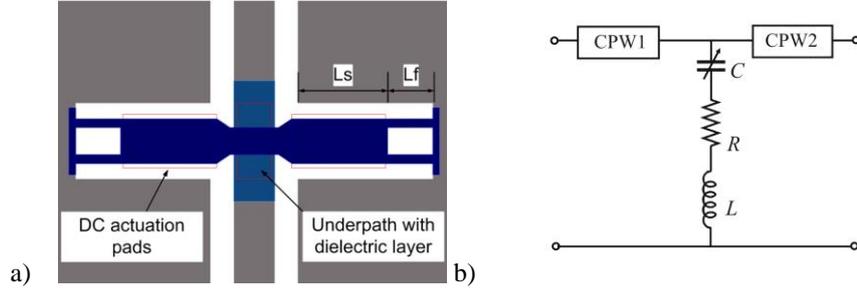
**Fig. 1** (a) Top-view of the realized switch and schematic of the cross-section [26] and (b) equivalent circuit of the RF MEMS switch RLC lumped element model

The inductance of the bridge and the fixed capacitance between signal line and bridge create a resonant circuit to the ground. The resonant frequency can be adjusted by varying the length of the bridge lateral dimensions. At the series resonance, the circuit acts as a short circuit to the ground. In a certain frequency band around the resonant frequency the transmission of the signal is suppressed.

An RF MEMS switch can be represented by a simplified equivalent circuit model, as shown in Fig. 1(b). It consists of the resistance $R$, the inductance $L$ and the capacitance $C$. Two coplanar waveguide lines, CPW1 and CPW2, are added with the aim of matching the obtained S-parameters with the S-parameters obtained by a full-wave analysis, having in mind that the reference planes for simulation and measurement are usually not defined directly at the membrane but a distance apart from it [26].

The switch resonant frequency is

$$f_{res} = \frac{1}{2\pi\sqrt{LC}}. \tag{1}$$

The switch capacitance in the membrane down-state case, considered in this case, is calculated from the layout using the following expression [3]:

$$C = \frac{\varepsilon_0 \varepsilon_r A}{t_d}, \tag{2}$$

where $\varepsilon_0$ is the dielectric permittivity, $\varepsilon_r$ is the relative dielectric permittivity, $t_d$ is the distance between the two plates forming the capacitor and $A$ is the surface of the plates. The capacitance is constant, because it does not depend on the bridge lateral dimensions. The other two elements, $R$ and $L$, depend on the bridge lateral dimensions $L_s$ and $L_f$. They can be obtained simultaneously by optimizations in a circuit simulator aimed to achieve the desired values of the equivalent circuit S-parameters. Alternatively, the inductance can be determined from the given resonance frequency as:

$$L = \frac{1}{4\pi^2 f_{res}^2 C}, \tag{3}$$

and then only the resistance is to be obtained by optimization in a circuit simulator. It should be noted that once the capacitance is determined, the extraction of the resistance

and the inductance should be repeated for each considered combination of bridge dimensions, which always requires new full-wave simulations to provide inputs for optimization. Following the approach proposed in [26], the lumped element scalability with the bridge lateral dimensions can be introduced by means of artificial neural networks, as will be described in the next section.

## 3. PROPOSED INVERSE MODELING APPROACH

To determine the switch lateral dimensions for the desired resonant frequency, and simultaneously to determine the corresponding equivalent circuit elements, a new inverse modeling approach is proposed in this work. The proposed approach is a hybrid approach combining neural modeling with a lumped element equivalent circuit. In other words, it is a combination of the black-box neural inverse modeling approach [19-21] and a modification of the scalable lumped element model proposed in [18]. Schematic diagram of proposed model is shown in Fig. 2. The aim of the first ANN (ANN 1) is to determine the length of the fingered part $L_f$ for the desired resonant frequency [19, 20, 22].

As described in the previous work, due to the fact that different combinations of the bridge solid and fingered parts' lengths may lead to the same resonant frequency value, it is not possible to use this approach to determine $L_s$ and $L_f$ simultaneously. Instead, the length of the solid part is considered as the inverse model input beside the resonant frequency. The second ANN (ANN 2) is used for modeling the relationship between the resistance and the bridge lateral dimensions $L_s$ and $L_f$. Unlike the model considered in [18] where the inductance dependence on the dimensions is modeled also by the ANN, having in mind that in the considered case the resonant frequency is known, it is possible to calculate the inductance by using the Eq. 3, assuming that the capacitance, which is constant and does not depend on the bridge lateral dimensions, has been determined previously. Therefore the value calculated by Eq. 2 is directly assigned to the capacitor in the equivalent circuit.
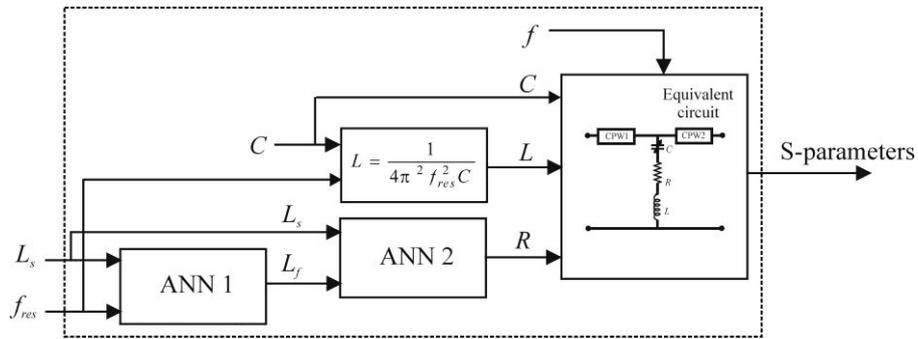


**Fig. 2** Proposed inverse modeling approach

The used ANNs are multilayered ANNs having one input layer, one output layer and one or more hidden layers [1]. Both ANNs have two input neurons and one output neuron. The inputs of the ANN 1 correspond to the bridge solid part length $L_s$ and resonant frequency $f_{res}$, and the output corresponds to the bridge fingered part $L_f$. For the training and

validation of ANN 1 it is necessary to have a set of samples consisting of a combination of dimensions and the corresponding values of the resonant frequency. That implies that simulations of the S-parameters in a full-wave simulator should be performed for each combination of the dimensions and the resonance frequency is determined as the frequency corresponding to the minimum value of the $S_{21}$ magnitude. The ANN 2 inputs correspond to the bridge lateral dimensions $L_s$ and $L_f$, whereas the output corresponds to the equivalent circuit resistance $R$. The training samples consist of the two considered lateral dimension combinations and corresponding resistances. Values of the resistance used for training are determined by optimization in a circuit simulator for the previously calculated capacitance and inductance, as described in Section 2. The flow chart describing the development of the proposed model is shown in Fig. 3. The optimization goal is to match the simulated resonant frequency (i.e. all scattering parameters) and the resonant frequency simulated in the full-wave simulator for the given combination of the dimensions.

   The implementation of ANNs in the equivalent circuit is done as follows. Each ANN is represented by a set of mathematical expressions describing the ANN transfer function. The expressions corresponding to the developed ANNs are implemented by means of a variable and equation blocks (VAR) on the equivalent circuit schematic. A VAR block inputs and outputs are the same as the inputs and outputs of the corresponding ANN. The output of the VAR block corresponding to the ANN 1 is led to the input of the VAR block corresponding to the ANN 2, whose output is further assigned to the resistance of the equivalent circuit.
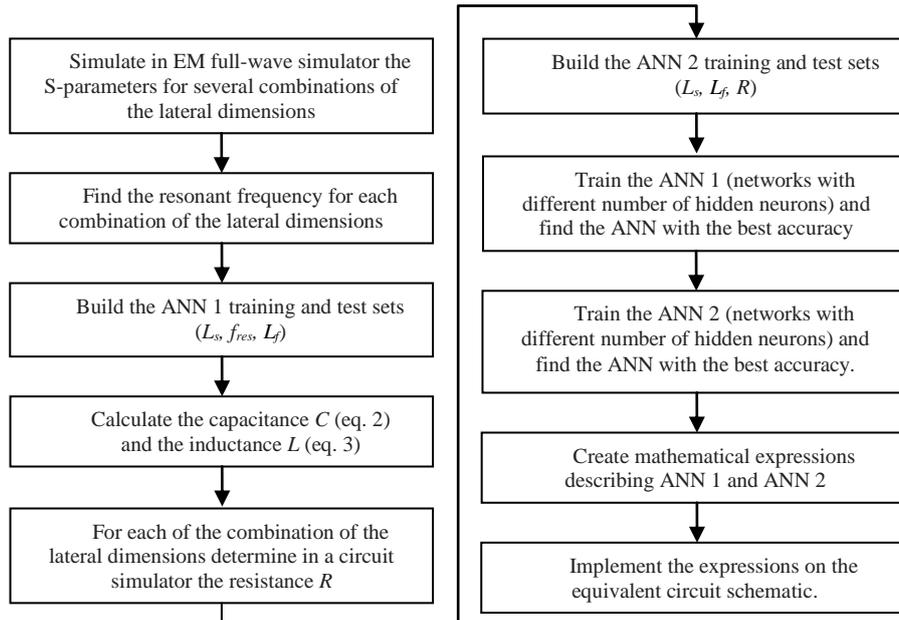


**Fig. 3** Model development flow chart

   The developed inverse model does not require additional simulations in the full-wave simulator or additional optimizations. For the desired resonant frequency and a given value of the bridge solid part length, by running the S-parameter simulations, it is possible to

simultaneously calculate the length of the fingered part, determine the corresponding elements of the equivalent circuit and simulate the S-parameters over the desired frequency range. As all the operations are performed in the circuit simulator, the whole process is done within seconds, which is significantly faster than performing optimizations in a full-wave simulator for determining the dimension and optimizations in a circuit simulator to determine the resistance.

## 4. NUMERICAL RESULTS

The proposed inverse model was developed for the following ranges of the switch geometrical parameters: $L_s$ from 50 μm to 500 μm, and $L_f$ from 0 μm to 100 μm. To prepare the data for the model development, the equivalent circuit elements $R$, $L$ and $C$ were determined for several different combinations of the lateral dimensions $L_s$ and $L_f$. The relative permittivity of Silicon dioxide is 3.9 and the dimensions contributing to the capacitance value in the down-state are $A = 13000$ μm$^2$ and $t_d = 0.1$ μm. Therefore, by using Eq. 2, the calculated capacitance in the down-state is 4.48695 pF. For each combination of $L_s$ and $L_f$, first the S-parameters were determined by full-wave simulations in Advanced Design System (ADS) Momentum software [29] and the resonant frequency was determined as the minimum of the $S_{21}$ parameter magnitude. Further, the combinations of the lateral dimensions and the resonant frequencies obtained by ADS simulations were used for training the ANN 1. The available dataset was divided into the training set used for the development of the ANNs and the test set used for the model validation. ANNs with different number of hidden neurons in one or two hidden layers were trained, because a prior determination of number of hidden neurons is not possible. The networks with the best test results were chosen as the final model. In this paper, the following notation of ANNs is used: ANN denoted with *N-H1-H2-M*, has *N* input neurons, *H1* and *H2* neurons in the first and second hidden layer, respectively, and *M* output neurons. In the Table 1, there are test results obtained by the best ANN 1 (2-15-15-1) for the input combinations whose values did not appear in the training set [19, 22].

**Table 1** RF MEMS switch inverse modeling results: $L_f$

| $L_s$ (μm) | $f_{res}$ (GHz) | $L_f$ (target) (μm) | $L_f$ (from ANN 1) (μm) | $L_f$ Abs. error (μm) | $L_f$ Relative error (%) |
|---|---|---|---|---|---|
| 5 | 22.78 | 25 | 24.9 | 0.1 | 0.4 |
| 75 | 19.17 | 65 | 65.4 | 0.4 | 0.6 |
| 75 | 17.92 | 85 | 85.3 | 0.3 | 0.3 |
| 100 | 17.5 | 75 | 73.6 | 1.4 | 1.9 |
| 200 | 13.13 | 85 | 86.8 | 1.8 | 2.1 |
| 350 | 11.67 | 25 | 23.4 | 1.6 | 6.4 |
| 350 | 10.83 | 65 | 62.2 | 2.8 | 4.3 |
| 400 | 10 | 85 | 87.4 | 2.4 | 2.9 |

The relative errors are in most cases less than 3%. However, the absolute difference of the predicted and expected values is less than 3 μm, which is already close to fabrication tolerances. More details about the development and validation of the mentioned inverse model can be found in [19, 22].

Further, the resonant frequency and the capacitance were used to determine the inductance for each combination of $L_s$ and $L_f$. The inductance is calculated by using Eq. 3 and achieved results are presented in Table 2.

In next step, the neural model for determining the resistance for the given dimensions (ANN 2) was developed. The target resistance values were obtained by optimization of the resistance value for each considered combination of the dimensions. CPWs of 50 Ω were used. Among the trained ANNs with different numbers of hidden neurons, the best results were obtained by ANN which has the structure 2-4-8-1. The resistance obtained by ANN 2 for the eight test combinations not used for the network training are shown in Table 2.

**Table 2** Extracted equivalent circuit elements

| $L_s$ (μm) | $L_f$ (from ANN 1) (μm) | $C$ (pF) | $f_{res}$ (GHz) | $L$ (pH) | $R$ (from ANN 2) (mΩ) |
|---|---|---|---|---|---|
| 75 | 24.9 | 4.48695 | 22.78 | 10.879 | 638.05 |
| 75 | 65.4 | 4.48695 | 19.17 | 15.363 | 739.45 |
| 75 | 85.3 | 4.48695 | 17.92 | 17.581 | 763.26 |
| 100 | 73.6 | 4.48695 | 17.5 | 18.435 | 764.92 |
| 200 | 86.8 | 4.48695 | 13.13 | 32.748 | 857.68 |
| 350 | 23.4 | 4.48695 | 11.67 | 41.455 | 908.49 |
| 350 | 62.2 | 4.48695 | 10.83 | 48.135 | 946.07 |
| 400 | 87.4 | 4.48695 | 10 | 56.457 | 977.75 |

To validate further the proposed hybrid inverse modeling approach, for the test combinations of the bridge dimensions, the calculated $C$, $L$ and $R$ were assigned to the corresponding equivalent circuit elements, and used for the S-parameter simulation.

The comparison of RF MEMS switch S-parameters simulated by the equivalent circuit and the S-parameters determined by the ADS momentum simulations shows a very good match. As an illustration, in Fig. 4 and Fig. 5 the insertion loss ($|S_{21}|$ in dB) and the return loss ($|S_{11}|$ in dB) are shown for two devices with different lateral dimensions: the first one having $L_s = 100$ μm and $L_f = 75$ μm, and the second device with $L_s = 350$ μm
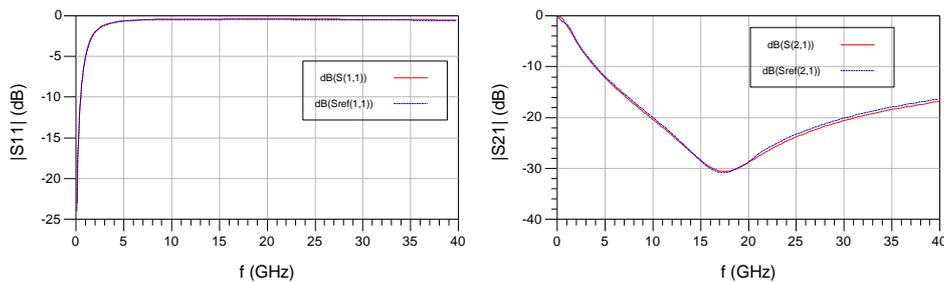


**Fig. 4** $S_{11}$ and $S_{21}$ of RF MEMS switch for $L_s = 100$ μm and $L_f = 75$ μm
(RLC model - red solid line, full-wave simulations – blue dashed line)
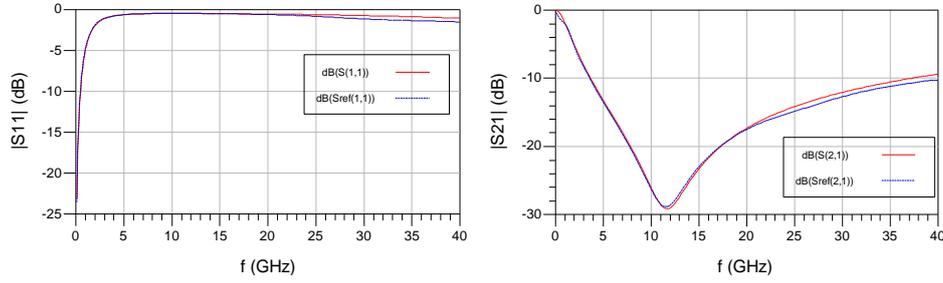
**Fig. 5** $S_{11}$ and $S_{21}$ of RF MEMS switch for $L_s = 350$ µm and $L_f = 25$ µm
(RLC model - red solid line, full-wave simulations – blue dashed line)

and $L_f = 25$ µm. As can be seen, in both cases the response of the equivalent circuit is almost identical to the reference response obtained by the full wave simulations, confirming the accuracy of the proposed approach. The results referring to the bridge with lateral dimensions $L_s = 350$ µm and $L_f = 25$ µm have been shown with the aim to show the results for the case where ANN 1 exhibits the biggest deviation between modeled and reference values. Even in that case, the circuit responses are almost identical and very close to the target values obtained by the full-wave simulations.

## 5. CONCLUSION

In this paper, a new approach to RF MEMS capacitive switch inverse modeling has been proposed. It is a hybrid approach combining artificial neural networks and a lumped element equivalent circuit model. The inverse approach proposed earlier by the authors aimed only to determine switch dimensions for the given resonant frequency. The inverse modeling approach proposed in this paper can be used to determine not only the necessary length of the bridge fingered part to achieve the given resonant frequency for the given value of the bridge solid part length, but also to determine the elements of the switch equivalent circuit in a full-wave simulator. After the ANNs composing the model have been developed, determination of the bridge fingered part length and the elements of the equivalent circuit are done straightforwardly without additional optimizations, making the process of inverse modeling very time-efficient. According to the obtained results, the accuracy of the determination of the bridge fingered part is within the fabrication tolerances. Moreover, the S-parameters simulated by using the equivalent circuit elements obtained by this approach match well the S-parameters obtained by full-wave simulations, confirming the accuracy of the equivalent circuit parameter extraction.

REFERENCES

[1]     Q. J. Zhang, K. C. Gupta, *Neural Networks for RF and Microwave Design*, Artech House, 2000.
[2]     M. Gad-el-Hak, *The MEMS Handbook Florida*: CRC Pres, 2002
[3]     G. M. Rebeiz, *RF MEMS Theory, Design, and Technology*. New York: Wiley, 2003.
[4]     G. M. Rebeiz, J. B. Muldavin, "RF MEMS Switches and Switch Circuits," *IEEE Microw. Mag.*, vol. 2, no. 4, pp. 59-71, December 2001.
[5]     Y. Mafinejad, A. Z. Kouzani, K. Mafinezhad, "Determining RF MEMS switch parameter by neural networks", *In Proceedings of the IEEE Region 10 Conference TENCON 2009*, 2009, pp. 1-5.
[6]     L. Michalas, M. Koutsoureli, E. Papandreou, A. Gantis, G. Papaioannou "A MIM capacitor study of dielectric charging for RF MEMS capacitive switches", *Facta Universitatis, Series: Electronics and Energetics*, vol. 28, no. 1, pp. 113-122, 2015.
[7]     M. Koutsoureli, L. Michalas, G. Papaioannou, "Assessment of dielectric charging in micro-electro-mechanical system capacitive switches", *Facta Universitatis, Series: Electronics and Energetics*, vol. 26, no. 3, pp. 239-245, 2013.
[8]     A. Napieralski, C. Maj, M. Szermer, P. Zajac, W. Zabierowski, M. Napieralska, Ł. Starzak, M. Zubert, R.Kiełbik, P. Amrozik, Z. Ciota, R. Ritter, M. Kamiński, R. Kotas, P. Marciniak, B. Sakowicz, K. Grabowski, W. Sankowski, G. Jabłoński, D. Makowski, A. Mielczarek, M. Orlikowski, M. Jankowski, P. Perek, "Recent research in VLSI, MEMS and power devices with practical application to the ITER and DREAM projects", *Facta Universitatis, Series: Electronics and Energetics*, vol. 27, no. 4, pp. 561-588, 2014.
[9]     I. Jokić, M. Frantlović, Z. Đurić, M. Dukić, "RF MEMS/NEMS resonators for wireless communication systems and adsorption-desorption phase noise", *Facta Universitatis, Series: Electronics and Energetics*, vol. 28, no. 3, pp. 345-381, 2015.
[10]   J. Iannacci and C. Tschoban, "RF-MEMS for Future Mobile Applications: Experimental Verification of a Reconfigurable 8-Bit Power Attenuator up to 110 GHz, " *Journal of Micromechanics and Microengineering (IOP-JMM)*, vol. 27, no. 4, pp. 1-11, Apr. 2017.
[11]   J. Iannacci, "RF-MEMS technology as an enabler of 5G: Low-loss ohmic switchtested up to 110 GHz", *Sensors and Actuators* A, vol. 279, pp. 624-629, 2018.
[12]   M. Donelli, J. Iannacci, "Exploitation of RF-MEMS Switches for the Design of Broadband Modulated Scattering Technique Wireless Sensors", *IEEE Antennas and Wireless Propagation Letters,* vol. 18, no. 1, January 2019.
[13]   E. Hamad and A. Omar, "An improved two-dimensional coupled electrostatic-mechanical model for RF MEMS switches", *J. Micromech. Microeng.,* vol. 16, pp. 1424, 2006.
[14]   L. Vietzorreck, "EM Modeling of RF MEMS," In Proceedings of the 7th International Conference on Thermal, Mechanical and Multiphysics Simulation and Experiments in Micro-Electronics and Micro-Systems, EuroSime 2006, Como, Italy, April 24-26, 2006, pp.1-4.
[15]   Z. J. Guo, N. E. McGruer and G. G. Adams, "Modeling, simulation and measurement of the dynamic performance of an ohmic contact, electrostatically actuated RF MEMS switch", *J. Micromech. Microeng*, vol. 17, pp. 1899-1909, 2007.
[16]   J. Iannacci, R. Gaddi, A. Gnudi, "A Experimental Validation of Mixed Electromechanical and Electromagnetic Modeling of RF-MEMS Devices Within a Standard IC Simulation Environment", *Journal of Microelectromechanical Systems*, vol. 19, no. 3, pp. 526-537, 2010.
[17]   http://www.coventor/mems-solutions/products/mems
[18]   T. Ćirić, R. Dhuri, Z. Marinković, O. Pronić-Rančić, V. Marković, L. Vietzorreck, "Neural Based Lumped Element Model of Capacitive RF MEMS Switches", *Frequenz,* vol. 72, no. 11-12, November 2018.
[19]   Z. Marinković, T. Ćirić, T. Kim, L. Vietzorreck, O. Pronić-Rančić, M. Milijić, V. Marković, "ANN Based Inverse Modeling of RF MEMS Capacitive Switches", In Proceedings of the 11th Conference on Telecommunications in Modern Satellite, Cable and Broadcasting Services (TELSIKS 2013), Serbia, October 16-19, 2013, pp. 366-369.
[20]   Z. Marinković, V. Marković, T. Ćirić, L. Vietzorreck, O. Pronić-Rančić, "Artifical neural networks in RF MEMS switch modelling", *Facta Universitatis, Series: Electronics and Energetics*, vol. 29, no 2, pp. 177-191, 2016.
[21]   T. Ćirić, Z. Marinković, O. Pronić-Rančić, V. Marković, L. Vietzorreck, "ANN approach for modeling of mechanical characteristics of RF MEMS capacitive switches - an overview", *Microwave Review*, vol. 23, no. 1, pp. 25-34, June 2017.
[22]   Z. Marinković, T. Kim, V. Marković, M. Milijić, O. Pronić-Rančić, T. Ćirić, L. Vietzorreck, "Artificial Neural Network based Design of RF MEMS Capacitive Shunt Switches", *Applied Computational Electromagnetics Society (ACES) Journal* , vol. 31 no. 7, pp. 756-764, July 2016.

[23] T. Ćirić, Z. Marinković, T. Kim, L. Vietzorreck, O. Pronić-Rančić, M. Milijić, V. Marković, "ANN based inverse electro-mechanical modeling of RF MEMS capacitive switches", In Proceedings of the XLIX Scientific Conference on Information, Communication and Energy Systems and Technologies (ICEST 2014), Niš, Serbia, June 25-27, 2014, vol. 2, pp. 127-130.

[24] Z. Marinković, A. Aleksić, T. Ćirić, O. Pronić-Rančić, V. Marković, L. Vietzorreck, "Inverse electro-mechanical ANN model of RF MEMS capacitive switches-applicability evaluation", In Proceedings of the XLX Scientific Conference on Information, Communication and Energy Systems and Technologies (ICEST 2015), Sofia, Bulgaria, June 24-26, 2015, pp. 157-160.

[25] T. Ćirić, Z. Marinković, M. Milijić, O. Pronić-Rančić, V. Marković, L. Vietzorreck, "Modeling of actuation voltage of RF MEMS capacitive switches based on RBF ANNs", In Proceedings of the 13th Symposium on Neural Networks and Applications (NEUREL), Belgrade, Serbia, November 22-24, 2016, pp. 119-122.

[26] S. DiNardo, P. Farinelli, F. Giacomozzi, G. Mannocchi, R. Marcelli , B. Margesin, P. Mezzanotte, V. Mulloni, P. Russer, R. Sorrentino, F. Vitulli, L. Vietzorreck, "Broadband RF-MEMS based SPDT", In Proceedings of the European Microwave Conference 2006, Manchester, Great Britain, September 2006.

[27] F. Giacomozzi, V. Mulloni, S. Colpo, J. Iannacci, B. Margesin, A. Faes, "A Flexible Fabrication Process for RF MEMS Devices", *Romanian Journal of Information Science and Technology (ROMJIST),* vol. 14, no. 3, 2011.

[28] D. Dubuc, K. Grenier, J. Iannacci, "RF-MEMS for smart communication systems and future 5G applications", in *Smart Sensors and MEMS -Intelligent Sensing Devices and Microsystems for Industrial Applications*, 2nd edition, Editors: S. Nihtianov, A. Luque, Chapter 18, Elsevier Ltd. Amsterdam, NL, pp. 499-539, March 2018.

[29] Advanced Design System 2009, Santa Rosa, CA: Electronic design automation software system produced by Keysight EEsof EDA.